Astron. Astrophys. 340, 483–496 (1998)

ASTRONOMY AND ASTROPHYSICS

An optical and near-IR spectroscopic study of the extreme P Cygni-type supergiant HDE 316285

D.J. Hillier[1], **P.A. Crowther**[2,⋆], **F. Najarro**[3,⋆⋆], **and A.W. Fullerton**[3,⋆⋆⋆,†]

[1] Department of Physics and Astronomy, University of Pittsburgh, 3941 O'Hara Street, Pittsburgh, PA 15260, USA
[2] Department of Physics and Astronomy, University College London, Gower Street, London, WC1E 6BT, UK
[3] Universitäts-Sternwarte München, Scheinerstrasse 1, D-81679 München, Germany

Received 29 May 1998 / Accepted 12 June 1998

Abstract. A detailed study of the Galactic P Cygni-type supergiant HDE 316285, based on high quality optical (AAT, MSO, CTIO) and near-IR (UKIRT, CFHT, CTIO) spectroscopy, is presented. As has been noted previously, its spectrum is dominated by H, He I, and Fe II P Cygni profiles. Emission lines due to N I, N II, [N II], O I, Na I, Mg II, Al II, Ca II, Si II, Si III, Fe II and [Fe II] can also be readily identified. Many of the metal lines are produced by continuum fluorescence. The rich N spectrum, the paucity of the O spectrum (only 2 O lines can be identified), and the apparent absence of emission due to C, strongly suggest that the atmosphere of the star is contaminated by CNO processed material. A comparison of the spectrum of HDE 316285 with P Cygni and He 3-519 is presented.

From a spectral analysis using the non-LTE atmosphere code of Hillier (1991), and assuming a distance of 1.85 kpc, our preferred model for HDE 316285 has the following parameters: $T_* = 15\,\mathrm{kK}$, $\log L_*/L_\odot = 5.44$, $\dot{M} = 2.4 \times 10^{-4}\,M_\odot\,\mathrm{yr}^{-1}$, $v_\infty = 410\,\mathrm{km\,s}^{-1}$, $E_{\mathrm{B-V}}$=1.81 mag, and H/He$\sim$1.5 by number. Due to the low degree of He ionization the derived H/He abundance ratio and mass-loss rate are strongly coupled. Models with H/He=10 to 0.5 are equally capable of explaining the H and He I spectrum provided the mass-loss rate is scaled according to the approximate formula $\dot{M} = 9.1 + 26.3(\mathrm{He/H} - 0.1) \times 10^{-5} M_\odot\,\mathrm{yr}^{-1}$. Preliminary work, however, indicates that a solar H/He ratio can be ruled out on the basis of line strengths of other species – particularly N, Mg, Al.

The stellar wind from HDE 316285 is more extreme than P Cygni with a performance number (= ratio of wind momentum to radiative momentum) 30 times greater. The low H/He abundance ratio and high N/He abundance ratio confirms that HDE 316285 is evolved.

Although we find no evidence in the literature for photometric variability, we find strong evidence for significant spectral variability. Because of the spectral variability, and because the stellar properties and chemical content of HDE 316285 are similar to known luminous blue variables (LBVs), we suggest that it is a LBV. Support for this contention comes from the detection by McGregor et al. (1988) of a cold circumstellar dust shell associated with HDE 316285. However HDE 316285, like P Cygni, could currently be in a relatively quiescent phase of its LBV life, exhibiting significant spectral variations but not undergoing major photometric outbursts similar to AG Car.

The mass loss of HDE 316285 is prodigious. In less than 10^5 years it will lose over 20 $M_\odot$. Even if HDE 316285 is not an LBV, it is obviously in an evolutionary phase of short duration.

Key words: stars: early-type – stars: individual: HDE 316285 – stars: mass-loss – stars: supergiants

1. Introduction

Massive stars play a dominant role in the ecology of galaxies in various ways. First, the bulk of their radiation is emitted in the far ultraviolet, thus providing the dominant source of ionization for the surrounding interstellar medium. Their powerful stellar winds also inject huge amounts of mechanical energy and chemically enriched material into their local environments, thereby influencing the chemical evolution of their galactic neighbourhoods. The least understood phase of the evolution of massive stars is the transition between H-burning O-type stars and He-burning Wolf-Rayet stars; current detailed evolutionary computations (e.g., Maeder 1991) indicate that the most massive stars pass through a phase identified with luminous blue variables (LBVs). During the brief, unstable LBV phase extreme mass loss peels off the outer H-rich atmosphere, to reveal the products of CNO-cycle burning. LBVs are characterised, at least during some epochs, by irregular photometric (0.5–2 mag) and spectral variations over timescales of decades.

Send offprint requests to: D. John Hillier

⋆ Visiting Astronomer, Cerro Tololo Inter-American Observatory, National Optical Astronomy Observatories, which are operated by the Association of Universities for Research in Astronomy, Inc., under contract with the National Science Foundation.

⋆⋆ *Present address:* CSIC, Instituto de Estructura de la Materia, Dpto. Fisica Molecular C/Serrano 121, 28006 Madrid, Spain

⋆⋆⋆ *Present address:* CAS, Department of Phys. and Astr., The Johns Hopkins University

† Visiting Astronomer, Canada-France-Hawaii Telescope, operated by the National Research Council of Canada, the Centre National de la Recherche Scientifique de France, and the University of Hawaii.

Table 1. Journal of principal optical and near-IR spectroscopic observations of HDE 316285. R_λ is the approximate size of a resolution element, expressed in $\mathrm{km\ s^{-1}}$.

Telescope	Spectrograph / Detector	Epoch	Range μm	R_λ $\mathrm{km\ s^{-1}}$
AAT	RGO/IPCS	Aug 1984	0.445–0.492	10
AAT	RGO/CCD	Aug 1985	0.600–1.000	10
AAT	RGO/CCD	Mar 1986	0.480–1.000	250
CTIO	2D-FRUTTI	Mar 1989	0.380–0.490	70
AAT	UCLES/1K Tek	May 1995	0.382–0.733	8
MSO	Coudé/2K Tek	Jun 1995	0.445–0.664	50
MSO	Coudé/2K Tek	Mar 1996	0.398–0.497	50
UKIRT	CGS4/ 58×62 InSb	Aug 1994	2.055–2.062	20
CFHT	FTS/InSb	Aug 1995	1.065–1.100	30
CFHT	FTS/InSb	Aug 1995	1.520–1.798	30
CFHT	FTS/InSb	Aug 1995	2.030–2.465	37
CTIO	IRS/256^2 InSb	Mar 1996	0.996–1.025	100
CTIO	IRS/256^2 InSb	Mar 1996	1.071–1.099	100

It is expected that detailed observations and analysis of individual evolved massive stars will improve our understanding of mass-loss and evolutionary properties of massive stars in general. One such object, which has been described as an LBV candidate, is the early-type Galactic supergiant HDE 316285 (CD-27° 119444, He 3$-$1482, MWC 272), which was discovered by Humason & Merrill (1922). Despite its close spectroscopic similarity to P Cygni, the properties of HDE 316285 have remained poorly determined, largely because of the high extinction associated with its location in the Galactic plane (Hillier et al. 1988). Although P Cygni has been intensively studied (Lamers et al. 1983, Pauldrach & Puls 1990, Najarro et al. 1997), HDE 316285 is sufficiently different that it can provide further constraints on the mass-loss properties, and evolution of massive stars.

In this paper we perform a detailed spectroscopic study and analysis of HDE 316285. New optical and near-IR spectroscopy of HDE 316285 are presented in Sect. 2. Spectral morphology, line identifications, and the spectral similarity of HDE 316285 to other LBVs, are discussed in Sect. 3. The distance of HDE 316285 and the amount of interstellar extinction are discussed in Sect. 4. Photometric and spectroscopic variability are examined in Sect. 5, using published observations, as well as our own data. A detailed, but preliminary, spectroscopic analysis of HDE 316285 is presented in Sect. 6. Finally, in Sect. 7, we discuss our results. The evolutionary status of HDE 316285 and the implications of our study for massive star evolution are also examined.

2. Spectroscopic observations

Table 1 summarizes the optical and near-IR spectroscopic observations of HDE 316285 that we have collected over the past decade, listing the relevant instrumentation, spectral range, and spectral resolution (which is expressed in $\mathrm{km\ s^{-1}}$, as determined from extracted arc spectra or the carriage travel in the case of FTS spectra). The majority of our optical spectroscopy was obtained at the 3.9m Anglo-Australian Telescope (AAT). Additional observations have been acquired at CTIO using the 1 m Yale telescope, and with the 74″ telescope at Mount Stromlo Observatory (MSO). Near-IR spectra have been obtained at the 3.8m UK Infra-Red Telescope (UKIRT), the 3.6m Canada-France Hawaii Telescope (CFHT), and the 4.0m Blanco telescope at Cerro Tololo Inter-American Observatory (CTIO).

2.1. Optical spectroscopy

Our principal optical spectra were obtained at the AAT, using either the RGO spectrograph or UCL echelle spectrograph (UCLES). High resolution observations were collected with UCLES, using the 31.6 lines $\mathrm{mm^{-1}}$ grating and a Tektronix 1K CCD. Other data were obtained with the RGO spectrograph and the IPCS or the RGO spectrograph and a GEC CCD. Complementary 74″ MSO observations were taken with the coudé spectrograph, 32 inch camera and 2K Tektronix CCD. All optical data were bias-corrected and flat-fielded within FIGARO (Meyerdierks 1993). RGO data were extracted and sky subtracted using FIGARO, UCLES echelle orders were optimally extracted using the software package ECHOMOP (Mills & Webb 1994), while Mount Stromlo coudé data were optimally extracted using PAMELA (Horne 1986). Photometric standards were observed to flux calibrate the stellar spectra. Once calibrated, the spectra were rectified using low order polynomials and measured within DIPSO (Howarth et al. 1995). At the request of the authors further optical observations were obtained, using 2D-FRUTTI on the 1m Yale telescope at CTIO, and reduced by Edward Fitzpatrick (see Fitzpatrick 1991 for details).

2.2. Near-IR spectroscopy

Near-IR spectroscopy was obtained using various telescopes and instruments (Table 1). In all cases, care was taken to remove atmospheric features through division by an appropriate standard star observed at approximately the same time and airmass.

High resolution UKIRT spectra were obtained with the cooled grating spectrograph CGS4, the 300mm camera and the echelle grating. Data were bias-corrected, flat-fielded, extracted and sky-subtracted using CGS4DR (Daly & Beard 1992). Subsequent reductions and analysis were carried out using FIGARO. In addition to the He I 2.058μm data included in Table 3, we also obtained fluxed low resolution ($R_\lambda \sim 400\,\mathrm{km\ s^{-1}}$) I, J, H and K-band data at UKIRT–CGS4, using the 75 l/mm grating. These served mainly to confirm the earlier, more extensive flux calibrated near-IR spectroscopy ($R_\lambda \sim 600\,\mathrm{km\ s^{-1}}$) obtained by McGregor et al. (1988) covering 1.05–3.5μm.

Spectra of HDE 316285 covering part of the J-band in the vicinity of He I 1.083μm and the entire H and K-bands with unapodized spectral resolutions between 8,200 (K band) and 10,000 (He I and H filters) were obtained with the Fourier

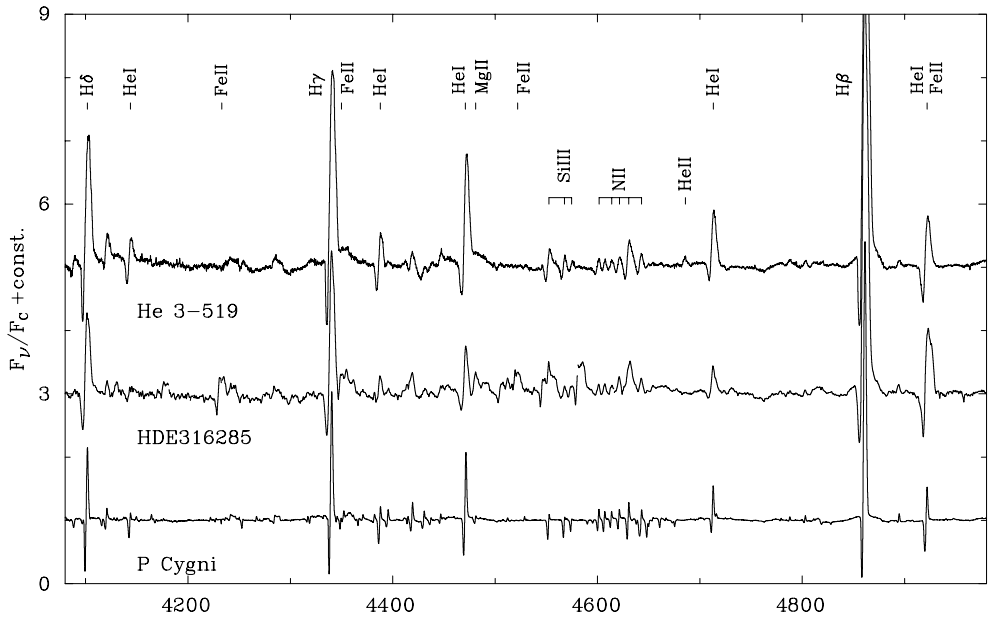

Fig. 1. A comparison of the blue spectra of P Cygni (Stahl et al. 1993), HDE 316285 and He 3–519 (Smith et al. 1994) that illustrates their very similar morphologies; see also Shore et al. (1990). For clarity successive spectra are offset by 2 continuum units.

transform spectrometer (FTS) at CFHT (Maillard & Michel 1982). Scans of the filters consisted of short integrations (100–200 msec) at a large number of path differences (1,536–5,120), which were chosen to avoid aliasing during the computation of spectra from the observed interferograms. Total scan times amounted to 5.1, 8.5, and 10.2 minutes for the He I, H, and K-filters, respectively. All scans were made with an internal phase modulation at 150 Hz in order to suppress the effects of detector and scintillation noise. For HDE 316285, each filter was scanned a number of times (4, 8, and 6 times for the He I, H, and K-filters, respectively). The resultant interferograms were inverted by means of the standard CFHT FTS reduction package, and the spectra obtained from individual scans were coadded in order to produce a single stellar spectrum with a high signal-to-noise ratio ($\sim$100). Subsequent processing steps included division by a lunar spectrum obtained at a similar airmass to the stellar spectrum in order to remove the filter function and most of the telluric contamination; multiplication by a high quality solar spectrum (obtained by manipulating machine-readable versions of the high-resolution solar atlases of Livingston & Wallace 1991 and Wallace, Hinkle & Livingston 1993) to remove the solar spectrum imprinted on the stellar data by the previous step; and rectification to a unit continuum.

Finally, spectra were obtained at the 4.0m CTIO Blanco telescope with the Infrared Spectrometer (IRS) together with the 210 l/mm grating in 4th (J–band) order. Two separate settings were used to cover He II 1.012μm (0.995–1.025μm) and He I 1.083μm (1.070–1.099μm). Data reduction was performed within IRAF[1] using pipeline tools developed at CTIO.

[1] IRAF is distributed by the National Optical Astronomy Observatories, which is operated by the Association of Universities for Research, Inc., under cooperative agreement with the National Science Foundation.

3. Optical and near-IR spectral morphology

The optical spectrum of HDE 316285 has previously been discussed by Merrill (1925), Swings & Struve (1941), Carlson & Henize (1979), Hillier et al. (1988), Shore et al. (1990) and Lopes et al. (1992). It is characterized by P Cygni profiles of the Balmer series, He I and Fe II, plus a continuum that appears very red. Features due to [Fe II], Na I, Ca II and possibly N II, Mg II and Si II have also been identified. Our extended wavelength coverage allows us to confirm the majority of these identifications, although definitive identification of the major contributors to some spectral features is complicated by the rich Fe II spectrum, the extreme non-LTE line formation, and the intrinsic width ($\sim$400 km s^{-1}) of the observed spectral features. Line identifications were based on a variety of sources. These include the papers on HDE 316285 by Swings and Struve (1941) and Carlson and Henize (1979), work on η Carinae by Hillier and Allen (1992) (which was based to a large extent on early work by Thackeray 1953, 1962), and the spectral atlas of P Cygni by Stahl et al. (1993). In addition, tables on atomic transition probabilities (Wiese et al. 1966, 1969), and the Grotrian diagrams of Bashkin and Stoner (1975) proved invaluable. The few remaining unidentified features are probably due to Fe II.

In Fig. 1 we present a comparison between high resolution blue spectra of HDE 316285, P Cygni (Stahl et al. 1993) and He 3–519 (Smith et al. 1994). Overall, HDE 316285 more closely resembles He 3–519 since their stellar winds produce features of comparable line strength and width, which are considerably stronger than analogous features in the spectrum of P Cygni. He 3–519 clearly shows the highest excitation of the three stars, with He II λ4686 emission. Next is P Cygni, which shows prominent Fe III emission but lacks He II λ4686, while HDE 316285 has only weak Fe III and also lacks He II λ4686. Line strengths of the principal optical and far-red spectral features in our AAT observations of HDE 316285 are presented in Table 2.

Table 2. Equivalent widths (W_λ) and peak intensities (P_λ) of the principal optical ($W_\lambda \geq 2$Å) and red ($W_\lambda \geq 5$Å) emission features in our AAT observations of HDE 316285. Wavelengths and equivalent widths are both given in Å; negative equivalent widths refer to principal P Cygni absorption components.

λ	Species	$W_\lambda^{\rm abs}$	$W_\lambda^{\rm em}$	$P_\lambda^{\rm em}$	λ	Species	$W_\lambda^{\rm abs}$	$W_\lambda^{\rm em}$	$P_\lambda^{\rm em}$
3890	He I (2) + Hζ	−1.4	4.5	2.0	6371	Si II (2)		1.6	1.3
3970	Hϵ	−2.4	4.0	1.8	6383	Fe II		3.1	1.3
4101	Hδ	−1.7	7.1	2.2	6456	Fe II (74)		2.3	1.2
4233	Fe II (27)	−0.7	2.7	1.3	6489	Fe II		4.5	2.0
4340	Hγ	−2.0	10.0	3.3	6563	Hα	−2.3	190.0	21.5
4354	Fe II (27)		3.7	1.4	6678	He I (46)	−1.5	8.2	2.0
4388	Fe II (27), He I (51)		1.0	1.3	7043	Al II (3)		2.9	1.2
4418	[Fe II](7F), Fe III(4)		2.5	1.3	7065	He I (10)		6.5	2.0
4471	He I (14)	−0.8	4.8	1.8	7155	[Fe II] (14F)		3.0	1.1
4481	Mg II (4)		1.8	1.3	7283	He I (45)		3.7	1.4
4522	Fe II (37,38)		2.3	1.4	7512	Fe II (73) +?		7.3	1.3
4552	Si III (2)		4.1	1.5	7876	Mg II (8)		6.3	1.4
4584	Fe II (38)		4.0	1.5	7896	Mg II (8)		8.6	1.5
4632	N II (5)		6.5	1.5	8232	Mg II (7)		13.4	1.3
4713	He I (12)		2.1	1.4	8291			4.5	1.2
4861	Hβ	−2.1	39.0	7.8	8445	O I (4)		9.2	1.6
4922	Fe II (42) + He I (48)	−2.0	7.3	2.0	8467	P17		5.8	1.4
5015	Fe II (42) + He I (4)	−2.3	11.1	2.4	8502	P16		6.1	1.4
5156	Fe III (5)		3.2	1.4	8545	P15	−0.7	5.6	1.5
5169	Fe II (42)	−1.0	10.7	2.3	8598	P14		7.9	1.5
5197	Fe II (49)		2.5	1.3	8665	P13 + Ca II (2)		7.4	1.6
5275	Fe II (49)		4.4	1.5	8682	N I (1)		7.1	1.5
5316	Fe II (48,49)	−0.5	5.7	1.6	8750	P12		9.5	1.7
5364	Fe II (48)		2.5	1.2	8863	P11		11.0	1.9
5666	N II (3)	−2.3	3.9	1.2	8925	Fe II		5.1	1.3
5755	[N II] (3F)		4.0	1.3	9015	P10		15.2	2.0
5876	He I (11)	−1.5	8.9	2.8	9069			9.5	1.3
5890	Na I (1)	−3.8	3.1	1.7	9126	Fe II		4.0	1.2
6243	Fe II (74) + Al II (10)		4.9	1.3	9229	Pζ + Mg II (1)		68.7	2.6
6317			2.5	1.2	9390	N I (7)		11.0	1.6
6347	Si II (2)	−0.3	3.4	1.4	9546	Pϵ		21.0	2.4

High resolution near-IR observations of HDE 316285 are presented in Fig. 2. As in the optical, spectra are characterized by strong H I and He I emission lines, together with permitted Mg II (2.137μm, 2.144μm) and Fe II features. Emission equivalent widths of prominent near-IR spectral features are presented in Table 3.

We now discuss lines of hydrogen and helium, CNO and heavy elements in more detail.

3.1. Hydrogen and helium

The Balmer lines show strong emission, together with blue shifted absorption. Swings & Struve (1941) indicate that the Balmer lines are in emission to at least H(12-2). Our high resolution spectra of Hα, Hβ and Hγ indicate that the absorption profile is almost black ($I_{\rm abs} \approx 0.1 I_c$ in IPCS data; ≈ 0.2 in UCLES data), and centered at a radial velocity of approximately $-330\,{\rm km\,s^{-1}}$. Both Hα and Hβ show broad blue and red wings extending to $\pm 1500\,{\rm km\,s^{-1}}$ which are attributed to electron scattering (Bernat & Lambert 1978). The Paschen, Brackett and Pfund series are strongly in emission, and can be followed until at least H(21–3), H(28–4) and H(29–5), respectively. Weak absorption components are present for at least some members of these series.

The He I lines also show strong P Cygni characteristics. In general, the observed He I profiles are narrower ($V_{\rm FWHM} \approx 270\,{\rm km\,s^{-1}}$) than the hydrogen lines ($V_{\rm FWHM} \approx 340\,{\rm km\,s^{-1}}$). Further, the minimum of the blue shifted absorption is centered at lower velocities ($V_0 \approx -270\,{\rm km\,s^{-1}}$) than in the hydrogen lines. Near-IR He I features also show strong P Cygni profiles (e.g. 2.0581μm, Fig. 2) when observed at sufficient spectral resolution.

No evidence is found for the presence of He II in our observations. The strongest He II features expected in our wavebands are λ4686 or 1.0124μm – both are absent.

3.2. CNO elements

Several multiplets belonging to N I and N II can be identified in our data. N II λ4601–43 is clearly present in the blue spectral

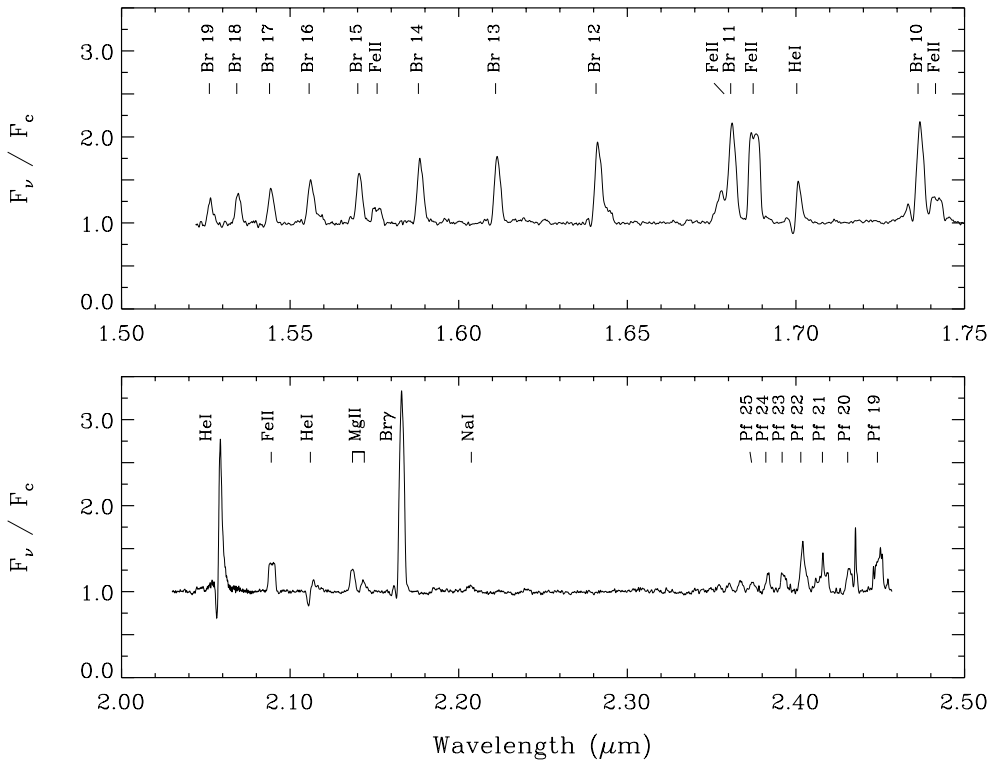

Fig. 2. H- and K-band spectroscopy for HDE 316285 obtained with CFHT-FTS, showing the presence of numerous H I, He I, Mg II and Fe II features, which were first identified in low resolution data by McGregor et al. (1988).

range, while [N II] λ5755 shows a square profile as illustrated in Fig. 3 and provides a useful abundance diagnostic. In addition, the N I spectrum is particularly rich, with at least 4 multiplets identifiable. The strongest N I line occurs at 8682 Å and has a central intensity greater than 50% above the adjacent continuum (Fig. 3).

No identifications of spectral features with oxygen in HDE 316285 have previously been reported. In our spectra only two oxygen lines, both belonging to O I can be unambiguously identified. O I $\lambda\lambda$7772–5 shows a P Cygni profile, while O I λ8446 is seen in emission and is attributed to a Lyβ fluorescence mechanism.

No emission (or absorption) features are identified with C I or C II, with C II at λ7231–6 – the strongest carbon feature in P Cygni – not visible in our high resolution spectra. Weak emission is seen in a low resolution spectrum, allowing a maximum EW of 1 Å to be placed on the strength of the C II feature. Confirmation of the weak feature with C II is not feasible as the optical spectrum of HDE 316285 is rich in weak emission features, and in addition the region around 7230 Å is affected by telluric absorption. While the weakness of C emission could be an excitation effect, the prevalence of N I and N II emission suggests that it is most likely due to a relatively low (i.e., below solar) C abundance.

3.3. Sodium–iron group elements

In addition to hydrogen, helium and CNO elements, several lines from heavier elements are also present in the optical and near-IR spectrum of HDE 316285. For example, the resonance doublet of Na I at $\lambda\lambda$5890–5896 is present (Fig. 3), as is λ4552–4575 Si III (Fig. 1).

Strong Mg II emission is found in the near-UV multiplet at $\lambda\lambda$2795–2803 (Shore et al. 1990), at λ4481 (M4, identification tentatively proposed by Carlson & Henize 1979), and in the near-IR multiplets 7877–7896 (M8), 8213–8235 (M7), and 9218-9244 (M1). Three further Mg II multiplets are detected in the IR – 10914–10952 (M3), 2.137–2.144 μm (5p-5s) and 2.404–2.413 μm(5p-4d). The 2.404 line explains the anomalous strength of H(22-5) seen in Fig. 2.

The strength of the optical and IR emission lines indicates that they cannot be formed by a pure recombination mechanism, or by collisional excitation, and so the most likely mechanism is continuum fluorescence. This continuum fluorescence occurs either via absorption from the ground state, or via absorption from the first excited state ($3p\,^2P^o$) which has an excitation energy of 4.43 eV. The viability of continuum fluorescence, via the $3p\,^2P^o$ state, is verified by the presence of P Cygni absorption on Mg II λ4481 (whose lower state is $3d\,^2D$).

Bruhweiler et al. (1982) suggest that a Bowen fluorescent mechanism is responsible for the Mg II emission observed in some Be stars. The fluorescent mechanism arises from a coincidence of Mg II $\lambda\lambda$1025.98, 1026.11 (5p-3s) with Lyβ λ1025.97. We can rule out Bowen fluorescence as being the most important mechanism in HDE 316285 using the following argument. In the Bowen process Mg II 2.137–2.144 μm is produced which in turn directly feeds $\lambda\lambda$8214–8235 (M7). Consequently the flux in the 2.137–2.144 μm feature should be greater than 0.38 (=0.82/2.14) times the flux in $\lambda\lambda$8214–8235 (the greater sign arises since the upper level of M7 can also decay to $3p\,^2P^o$).

Table 3. Emission equivalent widths (W_λ in Å) and peak intensities (P_λ) of the principal near-IR ($W_\lambda \geq 10$Å) features in our CTIO, UKIRT and CFHT observations of HDE 316285 (quantities in parentheses are from low resolution UKIRT data or McGregor et al. 1988).

λ (μm)	Species	W_λ	P_λ
0.9997	Fe II	28	2.5
1.0053	Pδ	30	3.4
1.0498		(26)	
1.0830	He I	47	4.8
1.0860		25	2.0
1.0911	Mg II	13	2.0
1.0938	Pγ	58	4.5
1.1125	Fe II	(16)	
1.2818	Pβ	(126)	
1.5556	Br16	13	1.6
1.5701	Br15	14	1.6
1.5881	Br14	22	1.9
1.6109	Br13	18	1.8
1.6407	Br12	29	2.0
1.6807	Br11	44	2.2
1.6879		40	2.0
1.7002	He I	10	1.5
1.7362	Brζ	32	2.3
1.7418		12	1.3
2.0581	He I	39	2.7
2.091	Fe II	16	1.4
2.137	Mg II	13	1.3
2.1665	Brγ	88	3.5
2.4029	Pf22 + Mg II	19	1.5
2.4157	Pf21	17	1.2
2.4307	Pf20	14	1.2
2.4483	Pf19	22	1.4

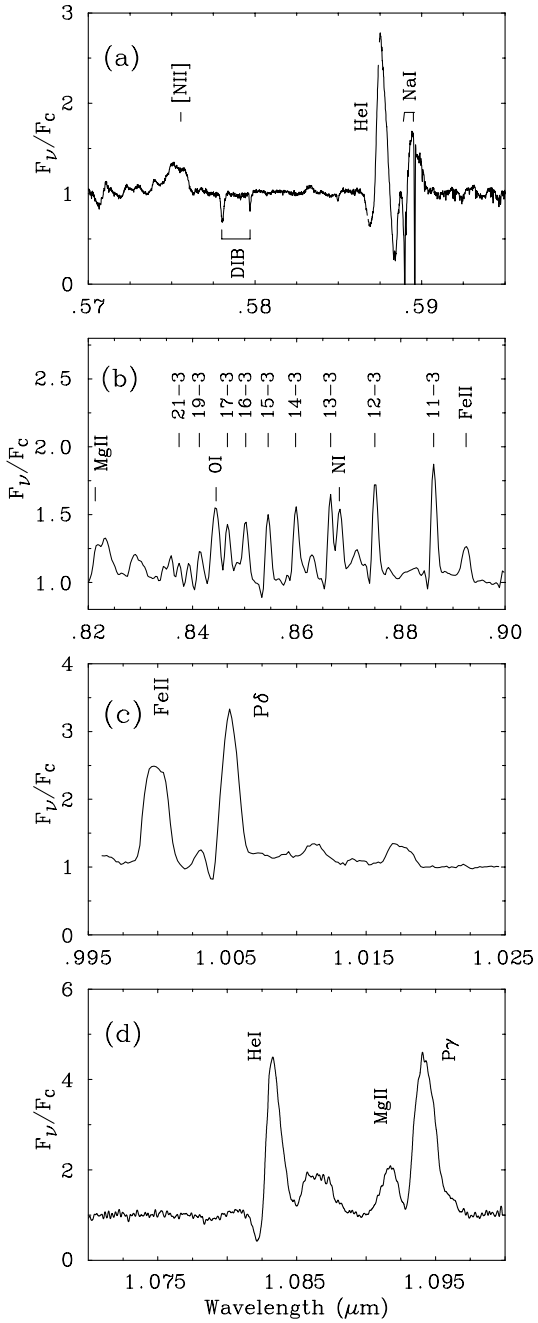

Fig. 3a–d. Selected spectra in the yellow–far-red regions for HDE 316285. **a** AAT–UCLES observations showing the N II λ5755, He I λ5876 and Na I λ5890–96 emission lines, plus $\lambda\lambda$5780-97 diffuse interstellar bands (DIBs). **b** AAT–RGO observations showing the high Paschen series lines. **c** CTIO–IRS observations of the 1μm region, including Pδ, with He II 1.0124μm absent. **d** CFHT–FTS observations of the He I 1.0830μm and Pγ profiles.

The observed flux in $\lambda\lambda$8214–8235 (M7) is at least a factor of 5 larger than would be predicted on the basis of the observed flux in 2.137–2.144 μm, and hence some other mechanism must be producing the observed emission.

Three multiplets of Al II are found to be definitely in emission – 6816–6837 (M9), 7042–7064 (M3), and 6226–6243 (M10). Their emission can also be explained via continuum fluorescence. In this case the important UV transitions have the metastable 3s3p ^{3}P^0 state as their lowest level, with the most important pump transitions occurring at $\lambda\lambda$1180–1220. The excitation energy of 3s3p^{3}P$^\circ$ is 4.65 eV. Other fluorescent lines are also possible, but there are several decay routes from the upper level and consequently the resultant lines are at the limit of detection. They might be detectable in high resolution and high signal-to-noise spectra, provided the spectral region is relatively blend free.

Swings & Struve (1941) proposed that the Ca II K line was in absorption in HDE 316285. Our observations confirm the identification, and show that it is a P Cygni type profile with the emission component weaker than the absorption component. The Ca II H line at 3968 Å is also present – absorption from this transition is clearly modifying the H(7-2) P Cygni profile at 3970.1Å. No other Ca II lines, including the $\lambda\lambda$8498–8662 triplet, can be identified in our spectra. While all three members of the Ca II triplet are severely blended with members of the Paschen series, the "relatively" smooth progression of the Paschen series, and the line centroids, suggest that the triplet can only be a minor contributor to the observed emission seen near the triplet wavelengths.

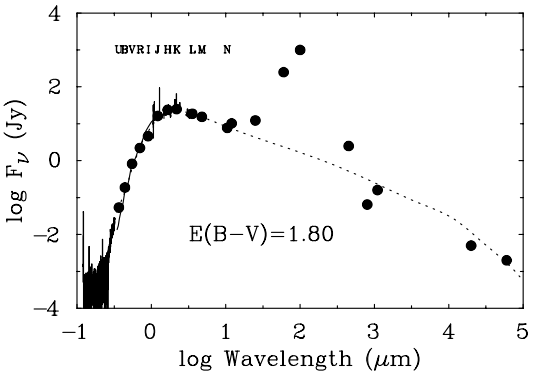

Fig. 4. Comparison between observed UV and near-IR spectrophotometry for HDE 316285, plus optical, IR, mm and radio broad-band photometry (McGregor et al. 1988; van der Veen et al. 1994; Shore et al. 1990) with our theoretical flux distribution, reddened by $E_{\rm B-V}$=1.8 assuming a standard Galactic extinction curve. The mid-IR excess is due to the presence of dust with characteristic temperature of $\sim$60K (McGregor et al. 1988).

As noted previously by Carlson & Henize (1979), the Fe II spectrum is extremely well developed, with many of the Fe II lines exhibiting P Cygni characteristics. The strongest optical Fe II features can be identified with multiplet 42 at $\lambda\lambda$4924, 5018, 5169, and all show strong P Cygni characteristics. The first two members of M42 are blended with He I lines, but the importance of Fe II to the feature near λ4924 can be gleaned easily from Fig. 1. From that figure we see that the emission ratio of He I λ4922 to He I λ4471 in HDE 316285 is anomalous compared with both P Cygni and He 3–519. Further, the absorption of the 4922 line is much stronger than that of He I λ4471. Other strong optical Fe II features can be attributed to the multiplet arrays M49, M73, and M74. Continuum fluorescence is probably the dominant mechanism which gives rise to the observed optical Fe II spectrum, as discussed by Brandi et al. (1987) for the peculiar emission line star GG Car.

Several forbidden Fe II lines are also observed in HDE 316285 (e.g. [Fe II] λ7135). Their weakness, and broad "flat-topped" profiles suggest that they are formed in the stellar wind, not in a circumstellar nebula. In addition to Fe II, several allowed Fe III transitions [e.g., $\lambda\lambda$5127, 5156 (M5)] can also be identified in the spectrum of HDE 316285. Overall, Fe II is more prominent than Fe III in HDE 316285, unlike in P Cygni, suggesting a lower ionization.

4. Interstellar extinction and distance

While it is generally accepted that the interstellar extinction towards HDE 316285 is extremely high, its exact value is uncertain. A wide range in values ($E_{\rm B-V}$=1.1–2) have been reported in the recent literature (Rao & Morrison 1989; Shore et al. 1990). Similarly, the distance of HDE 316285 remains poorly constrained, with estimates ranging from 1 kpc (van der Veen et al. 1994) to 3.4 kpc (Shore et al. 1990). Since the derived intrinsic properties of HDE 316285 depend critically on reddening and distance we now attempt to obtain more reliable determinations.

Interstellar reddenings are commonly determined by combining observed colours with estimates of intrinsic colours. However, these can be extremely inaccurate for stars with peculiar spectral appearances, such as HDE 316285. In addition, since strong emission features are observed in the optical spectrum of HDE 316285, broad-band Johnson photometry may suffer from line contamination effects. Shore et al. (1990) estimated (B−V)$_0$=−0.21 mag from the Q-method, which implied $E_{\rm B-V}\sim$2. Meanwhile, Rao & Morrison (1989) suggested $E_{\rm B-V}\sim$1.1 based on their estimate of (B−V)$_0$=+0.6 mag. Preempting the result of our model analysis in Sect. 6 we obtain a (line free) intrinsic colour of (B−V)$_0$=−0.08 mag, implying $E_{\rm B-V}$=1.86 since B−V=1.78 mag (Shore et al. 1990).

We also attempted to use the diffuse interstellar bands (DIBs), observed in our AAT-UCLES spectrum of HDE 316285 in order to estimate its reddening, since their strengths are considered to be closely related to the interstellar extinction (Herbig 1995). From the equivalent widths of DIBs at λ5797 and λ6614 relative to those in HD 183413, we obtain $E_{\rm B-V}$=0.88$\pm$0.1 mag, in very poor agreement with our more accurate determination, suggesting the presence of dark interstellar clouds along its line-of-sight.

Since the above determinations suffer from important deficiencies, we have carried out a comparison between the observed UV to IR energy distribution of HDE 316285 with a theoretical energy distribution, that results from our spectroscopic analysis, as shown in Fig 4. Optical and IR photometry is taken from Cohen & Barlow (1975), van der Veen et al. (1994), while supplementary UV, IR and radio spectroscopy is taken from Swings (1981), McGregor et al. (1988) and Shore et al. (1990). The strong infrared excess observed in HDE 316285 is due to a dust shell, whose properties have been studied by McGregor et al. (1988) and van der Veen et al. (1994). Our optimum fit to the overall energy distribution leads to a reddening of $E_{\rm B-V}$=1.8$\pm$0.05 mag.

Obtaining reliable distances to peculiar galactic field stars is notoriously difficult. In general, we could derive an approximate distance for a particular star by comparing its interstellar extinction to other nearby stars whose distance is known. In some cases we could compare the systemic velocity of interstellar absorption lines to the standard galactic rotation curve. Unfortunately, HDE 316285 lies towards the galactic center, preventing this.

Given our inability to constrain the distance we assume that HDE 316285 lies at an approximate distance of 2 kpc. Rather than fine tune each model to match the observed fluxes for a distance of 2 kpc exactly, we derive a "distance" for each set of model parameters, and this distance is quoted with our results. To scale the stellar parameters of HDE 316285 (discussed in Sect. 6) to other distances we can use the following proportionalities:

$$\begin{array}{ll} \dot{M} \propto d^{1.5} & \\ R_* \propto d & [d^{1.05}] \\ L \propto d^2 & [d^{1.79}] \\ T_{eff} \propto d^0 & [d^{-0.08}] \end{array}$$

These were found to hold for WN stars by Schmutz et al. (1989), and should provide reliable conversions for changes in distance of a factor 2 or less. The values in square brackets give the scalings found by Najarro et al. (1997) for P Cygni, which preserve its spectrum, but not the UV energy distribution. Thus while the uncertainty in distance limits our ability to place HDE 316285 accurately in the H-R diagram, it does not limit the validity of our spectral analysis.

Note that if we had assumed that the luminosity of HDE 316285 is comparable to that derived by Najarro et al. (1997) for P Cygni (i.e., $\log L/L_{\odot}$ = 5.75) the implied distance for HDE 316285 would be 2.6 kpc. Given the qualitative differences in the spectra of the 2 stars, however, there is little reason to suppose such an assumption is valid. The mass loss rate of HDE 316285 is, for example, an order of magnitude higher than for P Cygni.

5. Spectroscopic and photometric variability

Since HDE 316285 closely resembles the LBV P Cygni, and LBV-candidate He 3–519 (Smith et al. 1994), it might be expected to exhibit spectroscopic or photometric variability. However, Merrill (1925) did not detect brightness variations (Δm$<$0.1 mag) in Harvard plates spanning the years between 1890 and 1918. This constancy is supported by recent photometry of Carlson & Henize (1979) who obtained V=9.02, Dachs et al. (1982) who reported V=9.11, and Shore et al. (1990) who measured V=9.1. The (B$-$V) colours observed by Dachs et al. (1982) and Shore et al. (1990) differ by 0.11 mag. Since no other recent optical photometry has been obtained for HDE 316285 we concur with Merrill (1925) that there does not appear to be any significant photometric variability for this star. Similarly, no variability is known from infrared JHK photometry (McGregor et al. 1988).

Very recently van den Ancker et al. (1998) have analyzed Hipparcos photometry of Herbig Ae/Be stars and other emission line stars. They flag HDE 316285 as a probable variable. We note that the range in variability is only 0.13 magnitudes (5 to 95 percentile), and hence the variability is marginal. It should also be noted that the spatial resolution of the observations is only 10 arcseconds, and that consequently the magnitude of HDE 316285 is affected by a nearby companion.

To search for spectral variability we have examined our data sets obtained over the past decade, and compared these with published spectroscopy. Such a comparison is hindered by the wide variety of instruments and instrumental resolutions used to obtain the data. Moreover blends, and the existence of electron scattering wings on strong lines, can cause problems with continuum placement. Despite these problems, our data strongly suggest that HDE 316285 is a spectroscopic variable. Significant variability is seen in both H emission lines, and some metal lines.

A tabulation of Hα equivalent widths is presented in Table 4 together with the epoch of observations. The EWs vary by up to a factor of 2. Such a variation seems too large to be explained by observational error. An error as large as 10% in the continuum location results only in an error of 30 Å in the EW. For our measurements the electron scattering wing has been included.

Table 4. Hα equivalent widths

Date	EW(Å)	Reference
May 1985	275	RGO/CCD
May 1987	195	Shore et al 1990)
Mar 1988	375	Lopes et al. (1992)
Jun 1991	300	Schulte-Ladbeck
May 1995	190	UCLES

Table 5. Hβ equivalent widths

Date	EW(Å)	Reference
Aug 1984	66	RGO/IPCS
Mar 1986	51	RGO/CCD
Mar 1988	41	Lopes et al. (1992)
Mar 1989	50	2D-FRUTTI
Jun 1991	49	Schulte-Ladbeck
May 1995	41	UCLES

We have also examined the Hβ EWs, and these are presented in Table 5. Significant variations are also seen in these data. A difference of 10 Å in the EW is significant – the errors on an individual measurement are less than a few Å, especially when made by the same person (and hence with the same biases in drawing the continuum). The 1984 spectrum was taken with the IPCS, a photon counting device, and hence there is some concern regarding possible coincidence corrections (which can go in either direction). However the Fe II λ4921 EW at this epoch is also larger than in the UCLES data, and this line, due to its weakness, will not be affected by any problems with coincidence corrections. In addition, the P Cygni absorption component on Hβ differs significantly in the two data sets.

The best evidence for spectral variability comes from a comparison of the 1995 UCLES observations with the 1989 CTIO observations. This comparison reveals that the emission components in the H lines (particularly Hγ, and later) are all weaker (by approximately a factor of 1.5) than in the CTIO observations (Fig. 5). Many of the metal lines are also weaker, although surprisingly, the He I lines are similar in the two data sets. While echelle data are notoriously difficult to rectify, we have re-examined the original extracted orders, and are convinced that the rectification could not explain the observed discrepancies. Likewise we do not believe there is a problem with the 2D-FRUTTI data. The reality of the variability is, we believe, confirmed by its nature; some features in the 2 data sets are very similar while other spectral features, both weak and strong relative to the continuum, show marked differences.

Based on our analysis of the data we are forced to conclude that HDE 316285 is a spectroscopic variable. The absence of photometric variability may be real, or could be a chance occurrence arising from the limited and sporadic photometric data set. The observed spectroscopic variations, while not sufficient

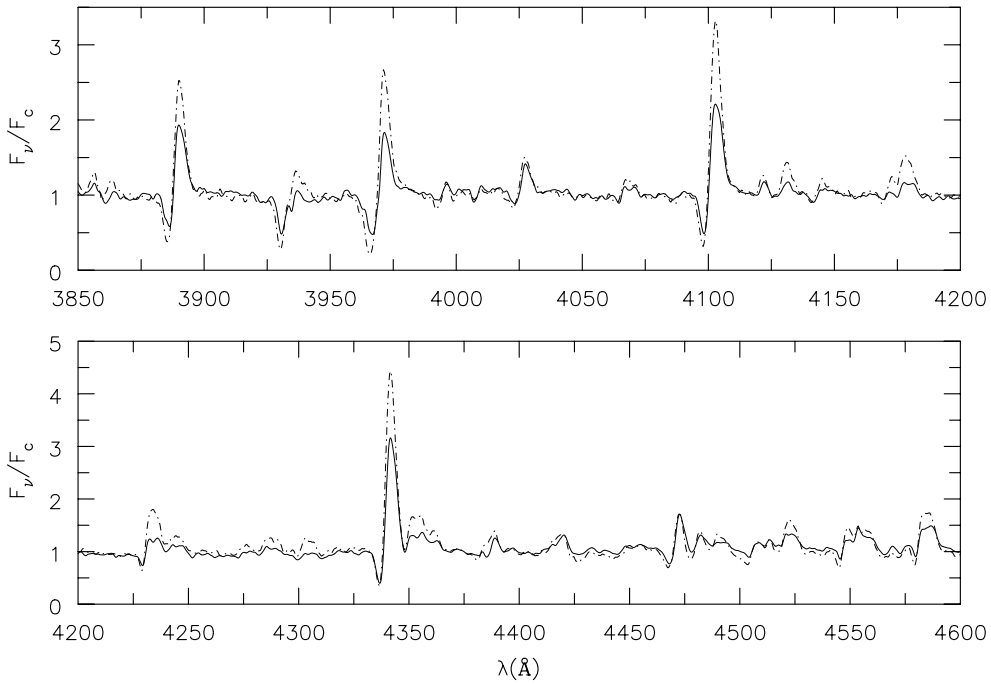

Fig. 5. Comparison between UCLES (May 1995) and 2D-FRUTTI (March 1989) data for HDE 316285. The UCLES data (solid line) has been smoothed to the approximate resolution of the 2D-FRUTTI data. Marked differences in the emission line strengths, particularly in H, are seen.

Table 6. Comparison of derived stellar parameters for HDE 316285 with those for P Cygni (Najarro et al. 1997), including the performance number $\eta \equiv \left(\dot{M} v_\infty\right)/\left(L_*/c\right)$. The H/He ratio is given by number; other symbols have their customary meanings.

Star	$T_\star$ (kK)	$T_{\rm eff}$ (kK)	$R_\star$ ($R_\odot$)	$R_{2/3}$ ($R_\star$)	$\log L/L_\odot$	H/He	$\log \dot{M}$ ($M_\odot$/yr)	v_∞ (km/s)	β	η	$(B-V)_0$	M_V
HDE 316285	15.3	10.1	75	2.3	5.44	1.5	-3.6	410	2.5	18	-0.08	-8.4
P Cygni	18.2	15.4	75	1.4	5.75	3.3	-4.5	185	2.5	0.5	-0.26	-8.0

to alter the star's classification, are large enough to affect spectral analyses. Future spectroscopic analysis should be based on data obtained at a single epoch. As in P Cygni, the observed changes in the spectrum of HDE 316285 might arise from ionization instabilities in the wind.

6. Spectroscopic analysis of HDE 316285

For stars with extended atmospheres such as HDE 316285, the usual assumptions of plane parallel geometry and local thermodynamic equilibrium (LTE) are totally inadequate. We therefore utilize the iterative technique of Hillier (1987, 1990) which solves the transfer equation in the co-moving frame subject to statistical and radiative equilibrium in an expanding, spherically-symmetric, homogeneous, steady-state atmosphere.

The present models include representative model atoms for H, He, and N only. Other species, such as O, Mg, Al, Na, Ca and Fe, which have been neglected, are being included in calculations currently being undertaken using the improved non-LTE code of Hillier and Miller (1998).

The spectroscopic analysis of HDE 316285 has proved to be extremely difficult – much more so than the recent spectral analysis of P Cygni undertaken by Najarro et al. (1997). This difficulty can be traced to several causes. First and foremost, the deduced He abundance and the mass-loss rate are strongly coupled. In particular, the lower the mass-loss rate the lower the He abundance required to match the He I line strengths (Sect. 6.1). Second, the velocity law plays an important role in determining the ionization structure. The velocity law thus provides additional degrees of freedom, which are difficult to constrain, for the model fits. Third, we have neglected Fe II, which will have a strong blanketing effect in the UV spectral region, and which potentially could cause systematic effects in our analysis. Finally, data from different epochs have been used, and as discussed earlier, we now find evidence for significant spectroscopic variability in HDE 316285.

6.1. Model results

In Table 6 we present our derived stellar parameters for HDE 316285, together with results for P Cygni from the recent detailed parameter study by Najarro et al. (1997), on which we have drawn heavily in the present work. In order to reproduce hydrogen and helium lines simultaneously it was necessary to use a slow velocity law with β=2.5, also obtained by Najarro et al. (1997) for P Cygni, and a photospheric velocity of $\sim$30 km s^{-1}. Nevertheless, we were unable to reproduce the observed profiles for high Paschen members and the precise shape of He I lines

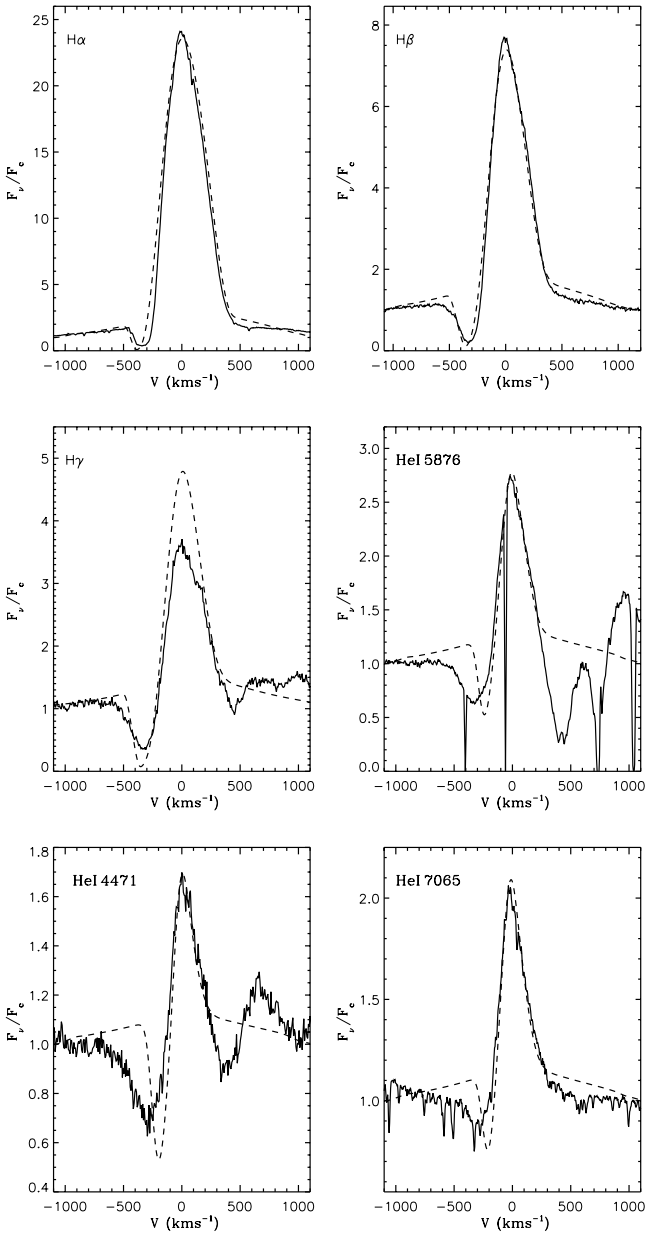

Fig. 6. Synthetic fits (dotted line) to Hα and selected He I lines. Solid lines are AAT–UCLES observations. The fit to He I λ5876 is affected by NaD on the red side. Similarly the fit to He I λ4471 is affected by Mg II λ4481 on its red side.

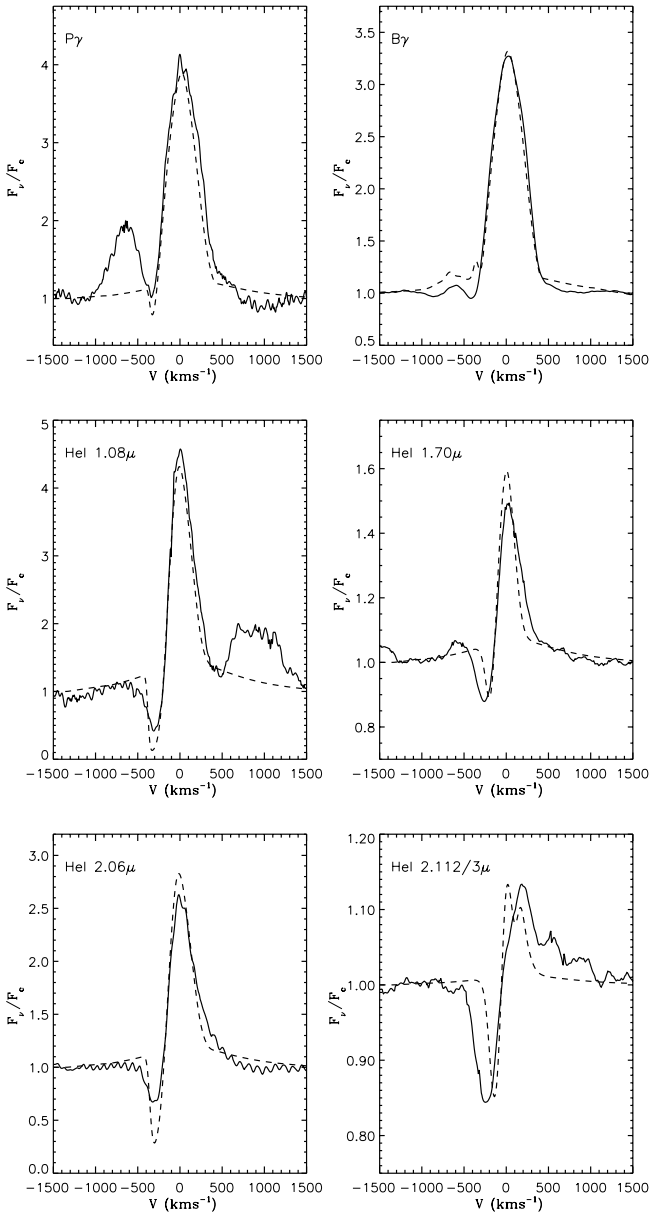

Fig. 7. Near-IR spectral fits (dotted lines) to CFHT–FTS data (solid lines) for HDE 316285.

(particularly the broad absorption components). Representative fits to optical line profiles are shown in Fig. 6 while additional fits to selected near-IR (CFHT) observations are presented in Fig. 7. As with P Cygni (Lamers et al. 1996), we anticipate that forthcoming ISO-SWS spectroscopy will allow an improved velocity distribution to be derived for HDE 316285.

Surprisingly, it is possible to match the H and He I spectrum of HDE 316285 using a range of H/He ratios [10 (i.e., solar) to 0.5] provided the mass-loss rate is scaled according to the approximate formula

$$\dot{M} = 9.1 + 26.3(\mathrm{He/H} - 0.1) \times 10^{-5} M_{\odot}\,\mathrm{yr}^{-1}. \quad (1)$$

The effect is illustrated in Table 7 where the parameters of four models, all capable of reproducing the H and He I observations to approximately the same accuracy, are tabulated. This model degeneracy can be traced to the low degree of He ionization. In HDE 316285, unlike P Cygni, He is predominantly neutral in the He I line formation zone. A decrease in He abundance can be compensated by a corresponding decrease in mass-loss which causes an increase in the He ionization. Note that the luminosity and effective temperature of all the models are very similar.

While a solar H/He ratio cannot be ruled out on the basis of the H and He I modeling, other considerations suggest that the ratio is substantially below solar. First, a model with a solar H/He ratio requires a very large N/He abundance ratio of 2.4×10^{-2} in order to explain the [N II] λ5754 emission; such

Table 7. Model parameter sets

Model #	H/He	N/He 10^{-3}	$\dot{M}$ 10^{-5}	L/$L_\odot$ 10^5
1	10	24	9.1	2.7
2	5	12	11.8	2.7
3	1.5	4.2	24	2.8
4	0.5	2.0	62	2.9

an abundance exceeds that expected from full CNO processing for solar metallicity by a factor of 6. Second, our preliminary calculations indicate that with the lower mass-loss rate of approximately $9 \times 10^{-5}\, M_\odot\, \mathrm{yr}^{-1}$ (Table 7) it would be difficult to produce the strength of emission lines due, for example, to Al II and Mg II. Third, the paucity of C and O lines in the spectrum of HDE 316285, and the richness of the N spectrum, suggests that we are seeing CNO processed material at the stellar surface. The nitrogen abundance for the preferred model is similar to that derived earlier by Hillier et al. (1988), and is consistent with that expected for a star of solar metallicity and equilibrium CNO abundances.

The present models can match the strength of [N II]5755, but underestimate the strength of the N II emission lines. To match the N II lines requires an increase in luminosity by a factor of 2 (which in turn would necessitate a higher H/He ratio). We attribute this discrepancy to the neglect of line blanketing, particularly by Fe II. The presence of strong emission due to Mg II, Al II, and Na I is more consistent with the lower luminosity model presented in this paper.

The estimate of the mass-loss (for the assumed distance and the adopted H/He ratio) is reliable provided clumping is unimportant. However the strength of the electron scattering wings, which can be unambiguously identified on many emission lines, are generally overestimated (e.g., Hα, Hβ, Fig. 6). This suggests that clumping is important, and consequently the mass-loss could be a factor of 2 lower. This issue will be addressed more rigorously in a subsequent paper.

The value of $410\,\mathrm{km\ s^{-1}}$ for V_∞ is based primarily on the width of the emission lines. On some lines (see, e.g., Fig. 6) there is evidence for blue-shifted absorption by material with velocities greater than $500\,\mathrm{km\ s^{-1}}$. This absorption may have a similar origin to the extended absorption (seen shortward of $V_{\rm black}$) in spectra of O and W-R stars (e.g., Prinja et al. 1990), and which is believed to arise from shocks in the stellar wind (see, e.g., Puls et al. 1993). Examination of weak forbidden lines (e.g., [Fe II] 5376), which should originate at electron densities of less than 10^8 cm^{-3}, confirms that V_∞ is approximately $400\,\mathrm{km\ s^{-1}}$. High signal-to-noise, moderate resolution observations, of additional forbidden lines might provide further constraints on V_∞ (and the velocity law), however it should be noted that most of the forbidden lines are weak, often blended, and can suffer from telluric absorption.

6.2. Comparison with previous results

All previous attempts to determine the stellar properties of HDE 316285 have relied on inadequate model assumptions, with the exception of Hillier et al. (1988). Shore et al. (1990) suggested a temperature of $T_{\rm eff}$ ∼23 kK, corresponding to their estimate of the intrinsic colour for HDE 316285. They estimated a distance of 3.4 kpc, which implied $\log\, L_*/L_\odot = 6.6$. In addition, Shore et al. suggested a huge mass-loss rate of $\dot{M}{\sim}4{\times}10^{-3}\, M_\odot \mathrm{yr}^{-1}$ (scaled to d=1.85 kpc) for HDE 316285 on the basis of their VLT radio observations. However, their 2–6 cm radio data are in reasonable agreement with our mass-loss estimate, a factor of 15 times lower. Note that H is *not* fully ionized in the radio emitting region (also true for P Cygni), and this must be taken into account when using the formula of Wright & Barlow (1975) to estimate the mass-loss rate.

From Table 6 it is apparent that the stellar properties of HDE 316285, while similar to those of P Cygni, are not identical. This is not surprising given the similarities and differences between their spectra. Both stars are highly evolved supergiants with slow winds ($V_\infty < 500\,\mathrm{km\ s^{-1}}$), and with effective temperatures less than 20,000 K. The biggest difference between the two stars is the mass-loss rate, and the efficiency of momentum deposition from the radiation field, as measured by the performance number η (=$c\dot{M}V_\infty/L$). A value of η in excess of 10 is, with the exception of Wolf-Rayet stars, unprecedented (e.g., Howarth & Schmutz 1992).

7. Discussion

The analysis of HDE 316285 raises many interesting questions:

1. Why is the performance number for HDE 316285 so large?
2. Why is continuum fluorescence so efficient in producing many of the metal emission lines seen in the spectrum of HDE 316285?
3. Why is it so difficult to match the high n-Paschen lines, and the absorption components on the He I lines?
4. What is the exact evolutionary status of HDE 316285, and how does it differ from that of P Cygni?
5. Is HDE 316285 a dormant LBV?

Below we will address some of these questions:

7.1. Wind performance number

The wind performance number (defined by $\eta = c\dot{M}V_\infty/L$) indicates the efficiency with which momentum from the radiation field is deposited into the wind. Values below 1 indicate that the wind momentum can be supplied through single scattering of continuum photons, while values in excess of 1 indicate that multiple scattering is extremely important. To obtain performance numbers of order 10 is extremely difficult, but not necessarily impossible (e.g., Lucy & Abbott 1993). It requires extreme line blanketing in the UV near the flux maximum, with approximately η optically thick lines every V_∞(Springmann 1994).

The performance number for HDE 316285 is approximately 15, and exceeds that of P Cygni by more than a factor of 30! A performance number in excess of 10 is usually only associated with W-R stars (see, e.g., tabulation by Hamann & Koesterke 1998). While HDE 316285 has a H/He ratio comparable to WNL stars, it is of a much lower excitation.

The large performance number (relative to P Cygni) might be attributable to the low wind ionization, and consequently the enhanced importance of Fe II in initiating and driving the mass flow. The importance of Fe, particularly Fe II in determining the wind properties of stars with temperatures less than 25,000 K has been discussed by Pauldrach & Lamers (1990).

Alternatively the high performance number might indicate that some other mechanism is responsible for, or at least influences, the mass-loss process. Rotation, for example, could be important. Langer (1997) notes that as a massive star evolves its rotation velocity at the surface will approach the critical value for breakup. Perhaps HDE 316285 is rotating near breakup. $V \sin i$ cannot be determined for HDE 316285, as no "photospheric" absorption lines are seen.

7.2. Line profile mismatches

The inability of our models to match all H and He I profiles might simply be due to the use of the wrong model; e.g., incorrect velocity law, our neglect of line blanketing, or the neglect of higher velocity material arising from radiation-driven wind instabilities. An interesting alternative is that the deficiencies might arise from the neglect of the effects of rotation.

HDE 316285 is polarized (3.1%, van Smith 1956), and given its large E_{B-V} value most of this is likely to be due to interstellar scattering. Low resolution spectropolarimetry observations by Schulte-Ladbeck (private communication), covering the range from 4000 to 7000 Å, were undertaken in 1991. Due to intermittent CCD controller problems the level of polarization cannot be determined reliably (although the value agrees with that of van Smith), however, there is evidence for a line effect (i.e., the polarization is not constant) in Hα which indicates the presence of intrinsic polarization. This would suggest that rotation might be important, or by analogy with P Cygni, it might indicate the presence of random structures in the wind (Taylor et al. 1991). High resolution and time resolved spectropolarimetry of Hα and other lines would be highly desirable, as there is increasing evidence that rotation plays a critical role in the evolution of massive stars (e.g., Meynet 1998), particularly for those stars which are evolving to the right on the H-R diagram.

7.3. Continuum fluorescence

As discussed in the text, many of the metal emission lines are produced by continuum fluorescence. It is of interest to ask why this process is so "efficient" in HDE 316285. The answer is related to both the dense wind of HDE 316285, and to atomic physics.

Consider continuum fluorescence in its simplest form in which an atomic level has 2 alternate decay routes, one in the optical (or IR), and the other in the UV. If the UV transition is optically thick, which will often be the case for a resonance transition or for a transition to a low lying level, this transition will absorb UV continuum photons. These photons may scatter in this transition (producing a UV P Cygni profile) or may be downgraded by emission in the optical transition. For the latter process to be efficient the branching ratio from the upper level, as set by atomic physics, should favor the optical transition. Alternatively the UV line must be sufficiently optically thick that a photon trapped in this line undergoes sufficient scatterings so that the probability of degradation into the optical line is significantly enhanced.

In HDE 316285 the dense wind and low ionization means that many transitions to the ground state and low lying states (with excitations of a few eV, for example) have significant optical depths. Further, species like Mg II often have favorable branching ratios so that the optical depths need not be large. In some cases the optical line is the preferred branch. Optical depth effects in the optical fluorescent lines are often unimportant (although exceptions are seen in the spectrum of HDE 316285), because the lower level of these transitions has a relatively large excitation energy.

Models with Mg II and Al II confirm the viability of the continuum fluorescence mechanism in HDE 316285.

7.4. The evolutionary status of HDE 316285

HDE 316285 shares many spectroscopic and physical similarities with other P Cygni type stars. They are all very luminous early B-type stars with extremely dense, slow stellar winds, and all show evidence for CNO processing. Their B-supergiant stellar temperatures range from ∼B4 for HDE 316285 to ∼B0 for He 3–519 (Smith et al. 1994).

HDE 316285 has an associated nebula, as evidenced from its circumstellar dust shell (McGregor et al. 1988; van der Veen et al. 1994). However, unlike P Cygni (Johnson et al. 1992) or He 3–519 (Smith et al. 1994) a detailed dynamical or abundance study has yet to be carried out. We note that neither nebular Hα nor [N II] λ6583 are observed in the AAT–UCLES spectrum, so that any ionized nebula is likely to be small. Indeed, the low degree of ionization of the central star (no H ionizing photons are produced due to the optically thick wind) together with its heavy interstellar reddening conspire to make such studies difficult. Ejecta-type nebulae are characteristic of a violent outburst of the central star in the recent past, and are commonly associated with LBVs and some WNL stars (e.g. Esteban et al. 1992). It remains to be determined whether the nebula around HDE 316285 is of such a type.

The mass-loss rate of HDE 316285 is prodigious. With the present mass-loss rate, it will take only 10^5 years for the star to lose over 20 $M_\odot$ of material. Clearly, HDE 316285 is in an evolutionary phase of short duration. Several lines of evidence indicate that this evolutionary phase is that ascribed to luminous blue variables. This evidence includes the spectral similarity of HDE 316285 to P Cygni, the presence of CNO processed material at its surface, spectroscopic variability, and the presence of

a nebula. The apparent absence of major photometric variations in HDE 316285 is not unusual for LBVs – P Cygni has been relatively quiescent since 1700 (Lamers 1986, de Groot 1989). Because of the importance of this stage to the understanding of massive star evolution, it is imperative that HDE 316285 be placed on long-term spectroscopic and photometric monitoring programs.

7.5. Evolutionary connections

What do P Cygni type stars look like at higher excitation? Their huge wind densities and surface elemental enrichments are comparable with late type WN (WNL) stars – indeed He 3–519 has been classified as a WN11 star by Smith et al. (1994), and has recently been shown to exhibit pure emission Balmer profiles (Crowther 1997). Recall that *bona fide* LBVs AG Car and R127 have also been observed to display WN11 spectral appearances (Smith et al. 1994; Crowther 1997). It is therefore tempting to suggest that HDE 316285 may evolve into a WNL star in the near future. Its surface chemical content (H/He$\sim$1.5, by number) is already comparable with most WNL stars (Crowther et al. 1995; Crowther & Smith 1997). Hillier et al. (1988) have previously suggested that HDE 316285 is rich in nitrogen and deficient in oxygen, a result confirmed by the present analysis.

In the future we will include ISO spectroscopy, examine the influence of iron group line blanketing, examine the influence of clumping, and determine metal abundances for HDE 316285. These will provide improved constraints on the precise evolutionary status of this unusual but extremely important star.

Acknowledgements. We appreciate the support of the staff at Mount Stromlo, Cerro Tololo, Canada-France-Hawaii and Anglo-Australian Observatories. We would like to extend special thanks to Linda Smith and Bruce Bohannan for co-observing some of our near-IR spectroscopy; Edward Fitzpatrick for obtaining the CTIO 2D-FRUTTI data, Peter McGregor for retrieving his near-IR observations; Regina Schulte-Ladbeck and Marilyn Meade for retrieving the spectropolarimetric observations; and David Bohlender for his outstanding support of our CFHT run, and for obtaining some of the FTS observations presented here. Financial support from NASA (STScI grant numbers 4450.01-92A and 5460.01-93A operated by AURA under NASA contract NAS5-26555 and grant NAGW-3828; DJH), PPARC (PAC), DGES under PB(6-0833) (FN), and DFG grant Pu 117/3–1 (AWF) is also gratefully acknowledged. The U.K. Infrared Telescope is operated by The Observatories on behalf of the Particle Physics and Astronomy Research Council. This research has made use of the SIMBAD database, operated at the CDS, Strasbourg, France. The NSO/Kitt-Peak FTS data used here were produced by NSF/NOAO.

References

Bashkin S., Stoner Jr. J.O., 1975, Atomic Energy Levels and Grotrian Diagrams. North-Holland Pub. Co.
Bernat A.P., Lambert D.L., 1978, PASP 90, 520
Brandi E., Gosset E., Swings J.-P., 1987, A&A 175, 151
Bruhweiler F.C., Morgan T.H., van der Hucht K.A., 1982, ApJ 262, 675
Carlson W., Henize K.G., 1979, Vistas Astr. 23, 213
Cohen M., Barlow M.J., 1974, ApJ 193, 401
Crowther P.A., 1997, In: Nota A., Lamers H.J.G.L.M. (eds.) Luminous Blue Variables: Massive Stars in Transition. PASPC 120, 51
Crowther P.A., Smith L.J., 1997, A&A 320, 500
Crowther P.A., Smith L.J., Hillier D.J., Schmutz W., 1995, A&A 293, 427
Dachs J., Kaiser D., Sherwood W.A., Nikolov A., 1982, A&AS 50, 261
Daly P.N., Beard S.M., 1992, Rutherford Appleton Laboratory, SUN27
Esteban C., Vilchez J.M., Smith L.J., Clegg R.E.S., 1992, A&A 259, 629
Fitzpartick, E.L., 1991, PASP 103, 1123
de Groot M., 1989, In: Davidson K., Moffat A.F.J., Lamers H.J.G.L.M. (eds.) Physics of Luminous Blue Variables. Kluwer, Dordrecht, p. 257
Herbig G.H., 1995, ARA&A 33, 19
Hamann W.-R., Koesterke L., 1998, A&A 333, 251
Hillier D.J., 1987, ApJS 63, 947
Hillier D.J., 1990, A&A 231, 116
Hillier D.J., Allen D.A., 1992, A&A 262, 153
Hillier D.H., McGregor P.J., Hyland A.R., 1988, In: Bianchi L., Gilmozzi R. (eds.) Proc. 2nd Torino Workshop, Mass Outflows from Stars and Galactic Nuclei. Ap&SSL 142, p. 215
Hillier D.J., Miller D.L., 1998, ApJ 496, 407
Horne K., 1986, PASP 98, 609
Howarth I.D., Schmutz W., 1992, A&A 261, 503
Howarth I.D., Murray J., Mills D., Berry D.S., 1995, Rutherford Appleton Laboratory, SUN 50.17
Humason M.L., Merrill P.W., 1922, PASP 34, 296
Johnson D.R., Barlow M.J., Drew J.E., Brinks E., 1992, MNRAS 255, 261
Johnson H.L., Wisniewski W.Z., Fay T.D., 1978, Rev. Mex Astron. Astrof. 2, 273
Lamers H.J.G.L.M., 1986, In: de Loore C.W.H., Willis A.J., Laskerides P. (eds.) Luminous Stars and Associations in Galaxies. IAU Symp. No. 116, Reidel, Dordrecht, p. 157
Lamers H.J.G.L.M., de Groot M., Cassatella A., 1983, A&A 123, L8
Lamers H.J.G.L.M., Najarro F., Kudritzki R.-P., et al., 1996, A&A 315, L229
Langer N., Hamann W.-R., Lennon M., et al., 1994, A&A 290, 819
Langer N., 1997, In: Luminous Blue Variable: Massive Stars in Transition. PASPC 120, p. 83
Livingston, W., Wallace, L., 1991, An Atlas of the Solar Spectrum in the Infrared from 1850 to 9000 cm^{-1} (1.1 to 5.4 microns), NSO Technical Report #91–001 (NOAO, Tucson)
Lopes D.F., Damineli Neto A., de Freitas Pacheco J.A., 1992, A&A 261, 482
Lucy L.B., Abbott D.C., 1993, ApJ 405, 738
Maeder A., 1991, A&A 242, 93
Maillard J.-P., Michel G., 1982, In: Humphries C.M. (ed.) Instrumentation for Astronomy with Large Telescopes. IAU Coll. 67, Reidel, Dordrecht, p. 213
McGregor P.J., Hyland A.R., Hillier D.J., 1988, ApJ 324, 1071
Merrill, P.W., 1925, ApJ 61, 418
Meyerdierks H., 1993, Rutherford Appleton Laboratory, SUN 86.9
Mills D., Webb J., 1994, Rutherford Appleton Laboratory, SUN 152.1
Meynet G., 1998, In: Howarth I. (ed.) Properties of Luminous Stars. PASPC 131, 96
Najarro F., Hillier D.J., Stahl O., 1997, A&A 326, 1117
Pauldrach A.W.A., Puls J., 1990, A&A 237, 409
Prinja R.K., Barlow M.J., Howarth I.D., 1990, ApJ 361, 607
Puls J., Owocki S.P., Fullerton A.W., 1993, A&A 279, 457

Rao S.M., Morrison N.D., 1989, BAAS 21, 743
Schmutz W., Hamman W-R., Wessolowski U., 1989, A&A 210, 236
Shore S.N., Brown D.N., Bopp B.W., et al., 1990, ApJS 73, 461
Smith L.J., Crowther P.A., Prinja R.K., 1994, A&A 281, 833
Springmann, U., 1994, A&A 289, 505
Stahl O., Mandel H., Wolf B., et al., 1993, A&AS 99, 167
Swings P., Struve O., 1941, ApJ 93, 349
Swings J.P., 1981, A&AS 43, 331
Taylor M., Nordsieck K.H., Schulte-Ladbeck R.E., Bjorkman K.S., 1991, AJ 102, 1197
Thackeray A.D., 1953, MNRAS 113, 211
Thackery A.D., 1962, MNRAS 124, 251
van den Ancker M.E., de Winter D., Tjin A Djie H.R.E, 1998, A&A 330, 145
van Smith E.P., 1956, ApJ 124, 43
van der Veen W.E.C.J., Waters L.B.F.M., Trams N.R., Matthews H.E., 1994, A&A 285, 551
Wiese W.L, Smith M.W., Glennon B.M., 1966, Atomic Transition Probabilities, Volume I Hydrogen through Neon, NSRDS-NBS 4
Wiese W.L, Smith M.W., Miles B.M., 1969, Atomic Transition Probabilities, Volume II Sodium through Calcium, NSRDS-NBS 22
Wallace L., Hinkle K., Livingston W., 1993, An Atlas of the Photospheric Spectrum from 8900 to 13600 cm^{-1} (7350 to 11230Å), NSO Technical Report #93–001 (NOAO, Tucson)
Wright A.E., Barlow M.J., 1975, MNRAS 170, 41